*J. Fluid Mech.* (1980), *vol.* 98, *part* 2, *pp.* 383–395
*Printed in Great Britain*


# Oscillatory flow in curved pipes. Part 1. The developing-flow case

By T. MULLIN† AND C. A. GREATED
Department of Physics, University of Edinburgh

(Received 15 May 1979)

The results of an experimental investigation of the entry, into a curved pipe, of the fully developed oscillatory laminar flow in a straight section are presented. Laser anemometry has been used to measure velocity profiles in the plane of the bend at various stations around a 180°-curved section. The flow development is found to depend upon both the frequency parameter of the flow and the amplitude of oscillation.

Results are presented for two values of the frequency parameter $\alpha$. The first is for small $\alpha$ where the flow can be considered quasi-steady and the flow development is found to proceed as in previous steady-flow studies. The other case, more extensively studied, is where $\alpha$ has a value such that both viscous and inertial effects play important roles in establishing the basic flow at different parts of the pressure cycle. The flow development process around the curve is found to be complicated, but a general trend is found and the results are explained in terms of those already established for steady-flow development in a curved pipe.

## 1. Introduction

The purpose of this paper is twofold. The experimental measurements were made at various stations around a curved pipe to determine at what stage the flow could be considered fully developed, and thus a comparison with the theoretical work reported in part 2 (Mullin & Greated 1980) could be made. A second aim was to investigate experimentally the development process using earlier theoretical and experimental studies for the steady flow case as a guide, to interpret the results.

The development of steady laminar viscous flow in a curved pipe is of interest in many physiological applications since the fully developed state is seldom attained in most real situations. The additional effect of pulsatility in the flow has received very little attention, although some recent theoretical work of Singh, Sinha & Aggarwal (1978) provides a first approach to the problem.

The treatment of the steady laminar-flow problem may be classified in terms of the entrance profile. The cases of uniform entry flow and fully developed pipe flow entering into a curved section have both been studied and general qualitative agreement between the analytical theories and experiment was found. Further, the numerical work of Humphrey, Taylor & Whitelaw (1977) provides quantitative agreement with their experimental work for fully developed square-duct flow entering a strongly curved section.

The main area of agreement between theory and experiment is in the prediction and discovery of an upstream influence on the flow before it enters the bend, owing to the curvature. This effect takes the form of an initial increase in axial shear stress at the inside of the curve in the entrance region as reported in the analytical work of

† Present address: Mathematical Institute, University of Oxford.

0022-1120/80/4450-1030 $02.00 

Smith (1976). This contrasts with the fully developed situation where the axial shear-stress maximum occurs at the outside of the bend. Smith found that, for either fully developed pipe flow or a flat entry profile, the upstream effects were the same. This upstream influence was eventually overtaken by centrifugally generated secondary flow from the outside of the curve to the inside around the walls of the tube leading to the fully-developed state. The point at which the cross-over in shear stress occurs was given by Smith as 1·51 pipe radii downstream of the inlet, independent of profile shape. The analytical work of Smith is only valid for very small curvatures.

Olson (1971) carried out an extensive experimental study on laminar developing flow in a curved pipe with both types of input profile, for a range of curvatures and flow rates. For a flat entrance profile, where the effects of viscosity were confined to the boundary-layer regions near the walls, the upstream influence was pronounced, the magnitude having a dependence on the curvature of the bend. The effect of the upstream influence was to cause the peak in the axial velocity profile, measured in the plane of the bend, to be displaced initially towards the inside of the curve. Eventually centrifugally driven secondary flow overcame this, with the maximum in the secondary flow occurring at around 60° round the curve for the range of curvatures and flow rates considered. The axial velocity maximum was then displaced towards the outside of the curve and the fully developed state was achieved.

He also investigated the case of a parabolic inlet profile where no upstream influence was reported, although detailed measurements were not presented for the beginning of the bend. It is stated however that for the parabolic profile the higher-velocity fluid deviates directly towards the outside of the bend over the full range of flow rates considered. Further, Olson found that for the parabolic entry profile the development length was longer and that the magnitude of the secondary flow was greater, indicating the important role of viscosity in the generation of the secondary flow field.

Another experimental study has been made by Agrawal, Talbot & Gong (1978) for a uniform entry profile. The results they present are in general agreement with Olson but in this study the effect of curvature on the magnitude of the upstream influence is more apparent. Finally, the numerical and experimental results of Humphrey *et al.* (1977) are in accordance with those of Olson for the parabolic input profile. In this case the profile development was measured extensively, starting at 2·5 diameters upstream of the bend. There is some evidence of a very small upstream effect but this is considered negligible and is not introduced into the numerical calculation of Humphrey (1977).

In a recent review of the entry problem, Yao (1978) reported on the work of Ito (1961), stating that Ito observed strong upstream influence for Poiseuille flow entering a curved pipe. Ito's experiments were carried out using fully developed turbulent pipe flow and it has been shown by Pratap & Spalding (1975) and Humphrey & Whitelaw (1976) that upstream influence effects, similar to those found in laminar flow with a flat entry, are observed. Humphrey and Whitelaw found experimentally that the secondary flow field induced by centrifugal effects was very much larger than the turbulence-stress-induced secondary flows.

The origin of the upstream influence was attributed to pressure influcnce travelling upstream by Pratap & Spalding. In the fully developed curved flow region a higher pressure exists at the outside of the curve than at the inside because of the greater centrifugal force acting on the fluid there. The pressure influence is allowed to travel upstream in their 'partially parabolic' finite-difference scheme and comparison with the results of parabolic solutions and experimental results shows that the effect was accounted for by this 'partially parabolic' procedure.

The analytical studies are successful in predicting the upstream influence but break down at a few pipe diameters into the curve. A further analytical study was made by Yao & Berger (1975) who had some success with the later regions of development for large-Reynolds-number flows, but did not find the upstream influence in the initial stages of the bend. There is clearly a requirement for more work on this problem where a matching of the two solution regions must be made.

This study will interpret the unsteady-flow results in terms of the established steady flow effects. For fully developed oscillatory flow in a straight pipe, it is known that viscosity has effect over different proportions of the cross-section of the pipe, depending upon a frequency parameter $\alpha = a(\omega/\nu)^{\frac{1}{2}}$, where $\omega$ is the radial frequency of oscillation of the flow and $\nu$ is the kinematic viscosity. For small values of $\alpha$ the flow is quasi-steady, whereas when $\alpha \geqslant 10$ a boundary-layer-type flow with an inviscid core prevails. Since, for the range of frequency parameters considered in this study $(0{\cdot}9 \leqslant \alpha \leqslant 5{\cdot}0)$, viscosity acts over varying amounts of the flow at different phase positions in the flow cycle, gross effects similar to those described in both types of the steady-flow studies are expected to be found.

A description of the experimental system used in this series of experiments will be given in § 2. The results are presented in § 3 in the form of velocity profiles measured at different phase positions and at various angular positions round the curve in the plane of the bend. Finally, discussion of the results is given in § 4.

## 2. The experimental system

The experiments described in this paper and in part 2 were performed in glass tubes with diameters in the range 3·6 mm to 6·2 mm with air as the working fluid. These small-diameter tubes were required so that the frequency parameter range of interest and small Reynolds numbers could be obtained reliably with practical flow rates and frequencies of oscillation. A schematic diagram of the oscillatory flow apparatus and the velocity-measuring system is shown in figure 1. Both of these are described in more detail in Mullin & Greated (1978). The pump, which was used to push air back and forth through the tubes in a sinusoidal manner, operated on the scotch-yoke principle. Flexibility was built into the system such that the frequency of oscillation and the volume flow rate could be varied independently. The pump could operate within its mechanical limitations over the frequency range 0·33–15 Hz with a peak-Reynolds-number (based on the peak mean velocity and the diameter of the tube) capability of around 200. Over a 17 hour test run it was found that its amplitude did not vary more than 2 % and the frequency drift was less than 1 %. Connexion between the models and the pistons was made using thick-walled plastic tubing chosen to be long enough to ensure that fully developed flow conditions could be obtained within the models. The series of pipes provided a totally enclosed system which was advantageous owing to the nature of the flow-velocity-measuring technique employed.

Flow velocities in the tubes were measured using a laser anemometer operating in the real-fringe mode and employing the photon correlation technique for signal analysis. The small diameters of the tubes required a system with very high spatial resolution. This was achieved in the following manner. Two parallel beams of slightly

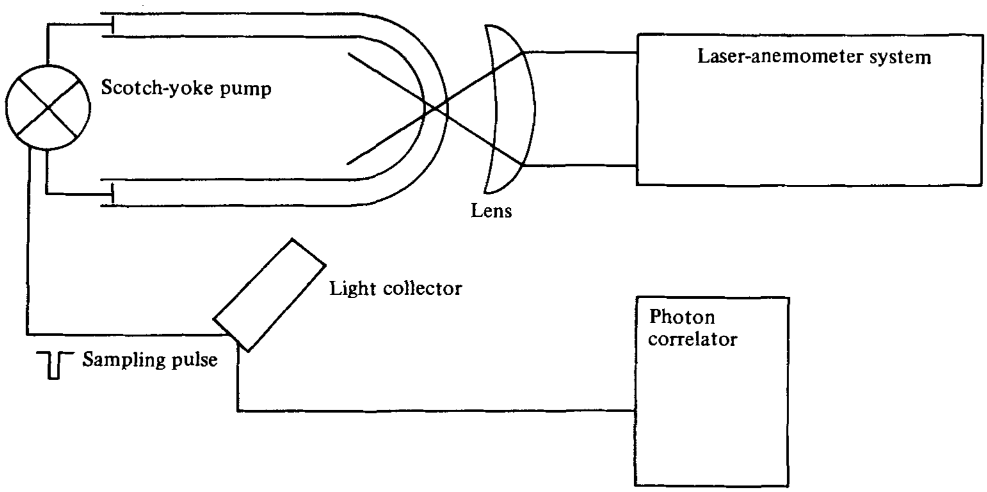


FIGURE 1. Schematic diagram of experimental system.

different optical frequencies were produced from a 15 mW He–Ne laser source using a beam splitter and phase-shifting device. The distance between the two beams was increased using a telescopic arrangement of lenses and they were then focused into the flow region through the glass walls of the tube using an $f$ 0·55 aspheric lens. A lens was also introduced between the laser and the beam splitter in order to ensure that the focused beams intersected at a position approximately coincident with their Gaussian waists. If the intersection point had not been coincident with the waists there would have been a distortion of the fringe pattern resulting in an additional Doppler broadening. The phase shifter was employed to produce a moving fringe pattern within the measuring region which superimposes a predetermined frequency shift on the Doppler signal. This allows one to determine the sense of the flow and also facilitates analysis of the correlograms. With this arrangement high-quality Doppler signals were obtained with a beam intersection angle of $60° 24'$, giving a measuring region of length $140 \mu m$ between $e^{-2}$ points on the intensity distribution in the direction of the optical axis. This gave good spatial resolution for the tubes used in this series of experiments since they ranged in diameter from 3·6 mm to 6·2 mm. The magnitude of the Doppler broadening caused by optical effects, i.e. the standard deviation of the power spectrum divided by the mean Doppler frequency, was calculated to be only 0·32 %.

With the photon-correlation method of signal analysis a count correlogram was generated for each phase position at a given measuring point, the measured velocity being the average of the velocities recorded over a number of cycles. Averaging was achieved by sampling the output of the photomultiplier at a known position in the piston cycle and accumulating the correlation products over many cycles to obtain a good estimate of the mean velocity. The sample width was set short to avoid time-dependent velocity-gradient problems and long enough to be practical. It was therefore chosen to be $\frac{1}{2}°$ per cycle. The digital method of light detection gives optimum optical sensitivity and thus only very low levels of light scattering were needed. Only small amounts of seeding particles were therefore required and, since the system was

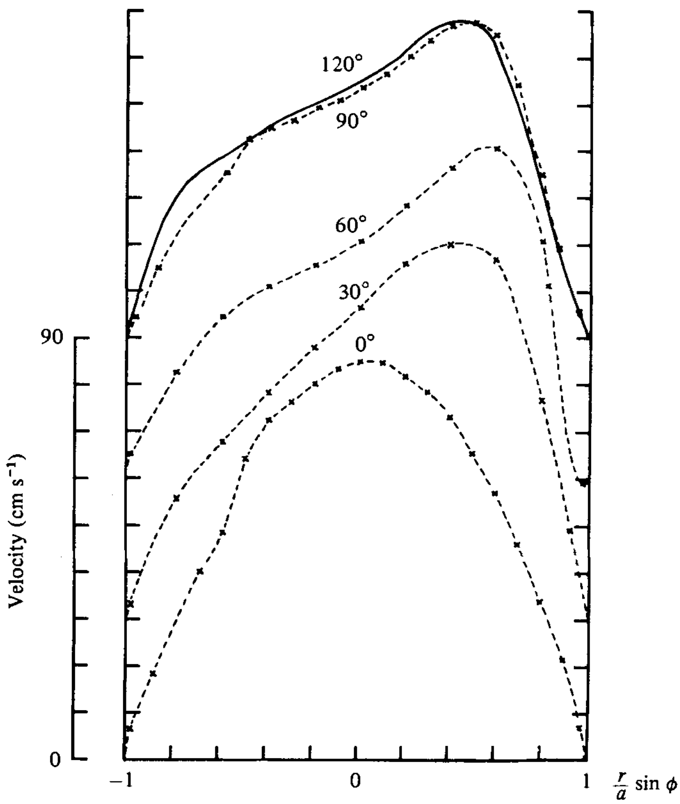


FIGURE 2. Series of velocity profiles measured at the 0 phase position with $\alpha = 0{\cdot}99$. Profiles measured at 0°–90° station show flow development and comparison with the 120° profile shows that the fully developed state is reached at $\approx 90°$ with $D = 64{\cdot}2$.

closed, these could be retained in the tubes for considerable periods of time, viz. around two hours.

The correlograms obtained in the experiments were converted to power spectra by applying a direct cosine Fourier transformation. This was a straightforward procedure as the correlator was wired on-line to a computer. It is known that, if the velocity gradient is linear across the measuring volume, then the peak frequency on the spectrum gives an accurate measure of the mean velocity, i.e. this frequency is the same as though all the light-scattering particles had traversed the volume at its centre. This criterion of linearity applies to a good approximation in these experiments because of the small size of the measuring volume in relation to the tube diameters. Considering the magnitude of the Doppler broadening and the accuracy with which the spectral peaks could be determined, it was estimated that the error in the velocity measurements was less than 1 %. It is also known that the spectrum width is related to the velocity gradient. This was used as a check on the results close to the edge of the tubes where gradients are high.

Since the relationship between mean velocity, i.e. piston velocity, and pressure gradient is known (Uchida 1956), all velocity measurements could be related to a particular phase position in the pressure cycle. The position of the measuring volume was located with a travelling microscope and, using sufficient seeding to make the

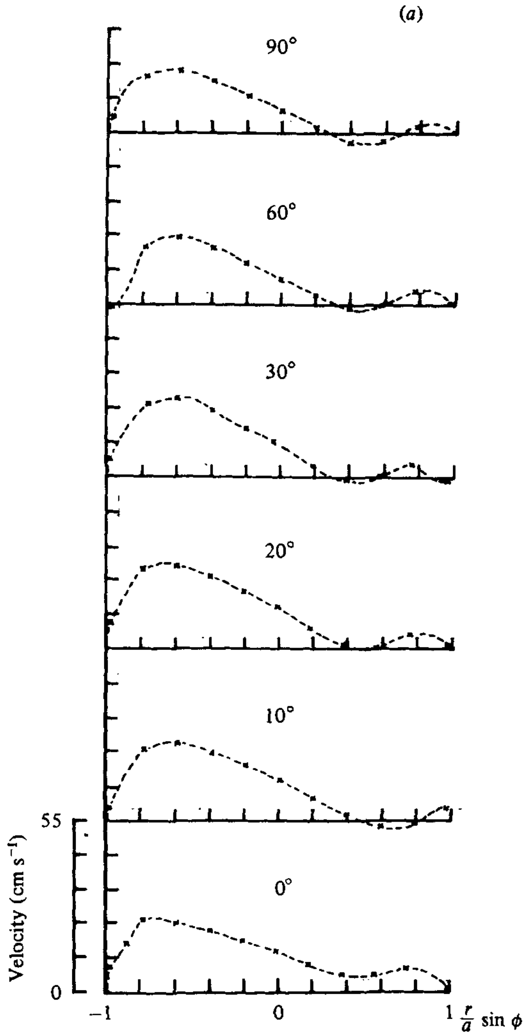


FIGURE 3 (*a*). For caption see p. 393.

volume visible, the tube traverse system was calibrated. Using this system 'instantaneous' axial velocity profiles were measured in both straight and curved pipes by traversing the tube using a precision optical traverse calibrated in 20 $\mu$m steps.

The results presented in this part of the paper were obtained in a U-tube of curvature $a/R = 1/7$, where $a$ is the radius of the tube and $R$ the radius of curvature of the bend. The curved section was manufactured by bending a 6·2 mm internal diameter, precision-bore Pyrex tube with wall thickness 1·5 mm. The skill of the glassblower was severely tested in making this model but after many trials a curved section was obtained, which maintained circularity to within 2 % around the curve.

Fully developed profiles were measured in the straight section of the U-tube, a distance around 10 diameters from the curve and these were reported in Mullin (1978). They show agreement with the exact solutions to the Navier–Stokes equations for an infinitely long pipe and were used to evaluate and calibrate the experimental system.

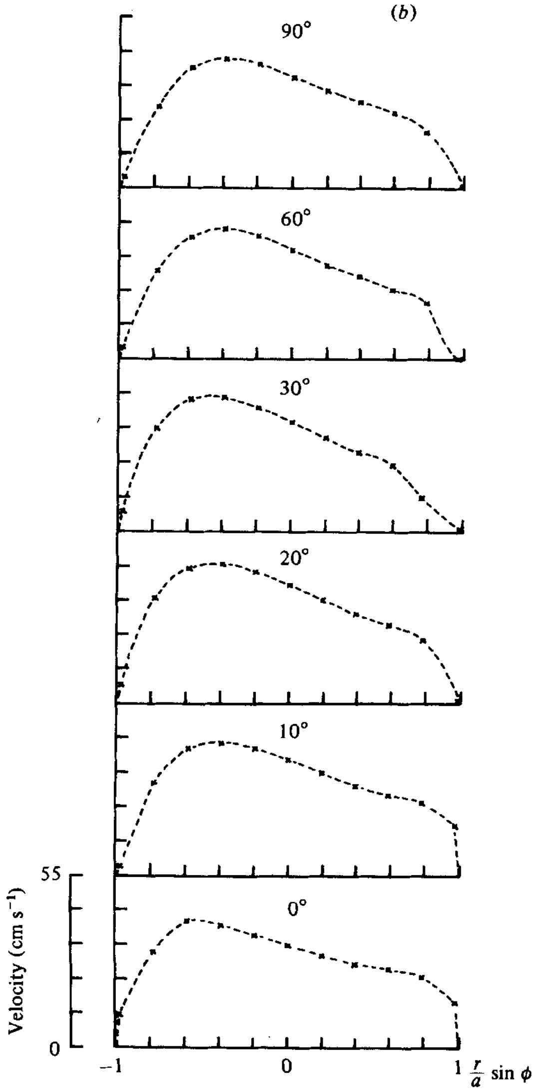


FIGURE 3 (*b*). For caption see p. 393.

## 3. Results

The results are presented in the form of velocity profiles measured in the plane of the bend. Each profile corresponds to a different phase position within a pressure cycle and also a fixed angular position around the curve. The phase position will be given in radians and the position round the curve in terms of degrees.

Profiles are presented for two values of the frequency parameter $\alpha = a(\omega/\nu)^{\frac{1}{2}}$, where $a$ is the radius of the tube, $\omega$ the angular frequency and $\nu$ the kinematic viscosity. The two cases presented are for small $\alpha$, where the flow is quasi-steady and viscous effects dominate, and moderate $\alpha$, where complex profiles arise due to the presence of both inertial and viscous forces.

The first set of profiles shown in figure 2 were measured at the 0 phase position with $\alpha = 0{\cdot}99$ and $D = 64{\cdot}2$ (peak $D = (2W_0\ a/\nu)\ (a/R)^{\frac{1}{2}}$, where $W_0$ is the peak

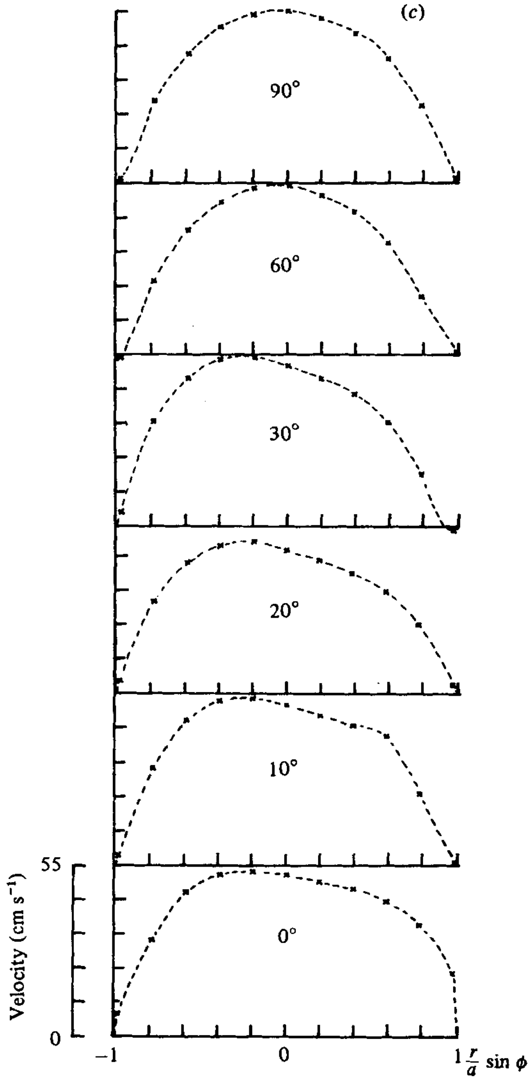


FIGURE 3 (c). For caption see p. 393.

instantaneous mean velocity, i.e. the velocity averaged over the tube diameter at the peak of the cycle, and $R$ is the radius of curvature of the bend). All profiles presented here are experimentally-determined ones. The crosses represent measured points and the dashed curves are cubic splines drawn through these points.

The results show that essentially fully developed conditions have been achieved by around 90° around the curve. The $D$ used in this experiment is the largest one employed in this series of tests and the results compare favourably with those presented by Olsen for $D = 75$. No observable upstream influence is found and the peak in the profiles drifts directly towards the outside of the bend under the action of the centrifugally derived secondary flow. The displacement of the peak in the profile reaches a maximum at around 60° which is in agreement with the steady-flow work of Olsen.

The next set of profiles shown in figures 3(*a*)–(*f*) illustrate the flow development when $\alpha$ is increased to 4·36. The profiles for the 0 and $\frac{1}{8}\pi$ phase positions show a very

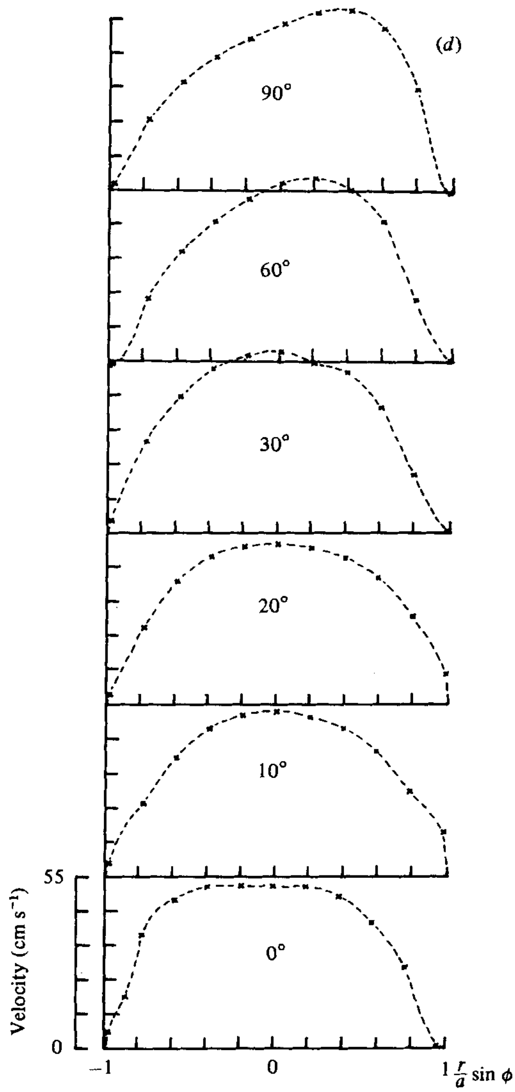


FIGURE 3 (*d*). For caption see p. 393.

strong upstream influence of the curvature at the entrance to the bend. This takes the form of a skew in the axial velocity profile such that the peak occurs at the inside of the bend. Secondary-flow effects do not play an important role and the skew in the profiles remains at the inside of the bend at all positions round the curve.

The effects of secondary flow first became noticeable at the $\frac{1}{3}\pi$ phase position. Again the inlet profile is initially skewed towards the inside of the curve but now this position is modified further around the curve by secondary flow action. The velocity profile is changed such that it is almost symmetric at position 90° round the curve. The most significant change in the velocity distribution occurs between 30° and 60° round the curve with little change between 60° and 90° indicating that fully developed conditions prevail.

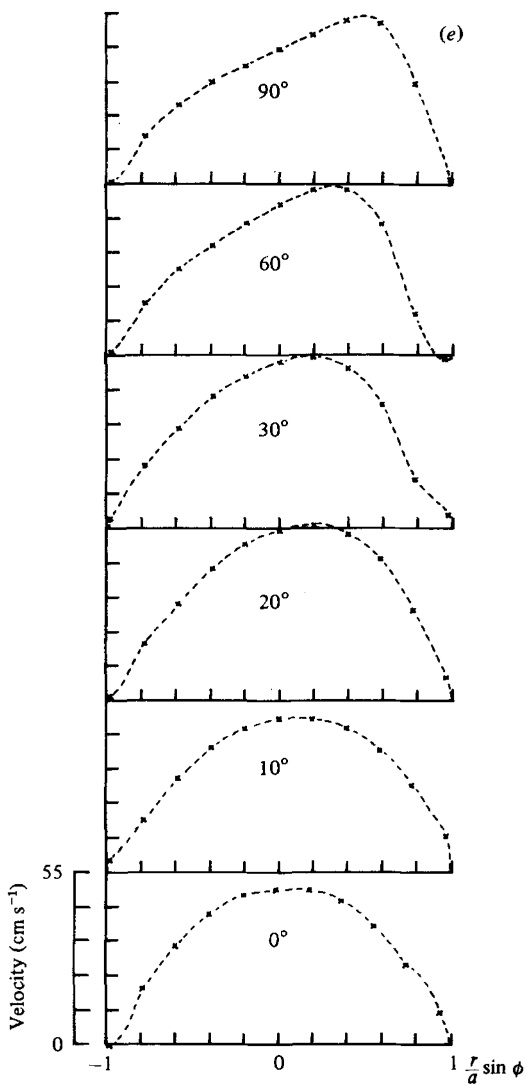


FIGURE 3 (e). For caption see p. 393.

At the $\frac{1}{2}\pi$ phase position the inlet profile is found to be only slightly affected by the downstream curvature and there is found to be only a small skew in the profile. The flow-development procedure is such that secondary-flow effects cause the peak in the profile to drift toward the outside of the curve. The effects do not become appreciable until around 60° round the curve, the development process being slow in the initial stages. At this position the flow may not be exactly fully developed at the 90° station, but since $D$ is around 39 then it is not expected to be far from the fully developed state.

The results presented here for this phase position do not agree with the fully developed theoretical results of part 2. In order to investigate this point further, a series of axial velocity profiles were measured at this phase position and at station 90° round the curve for a range of $D$s. These results are shown in figure 4 and they indicate that the effects of secondary flow become appreciable when $D \gtrsim 26$. Thus

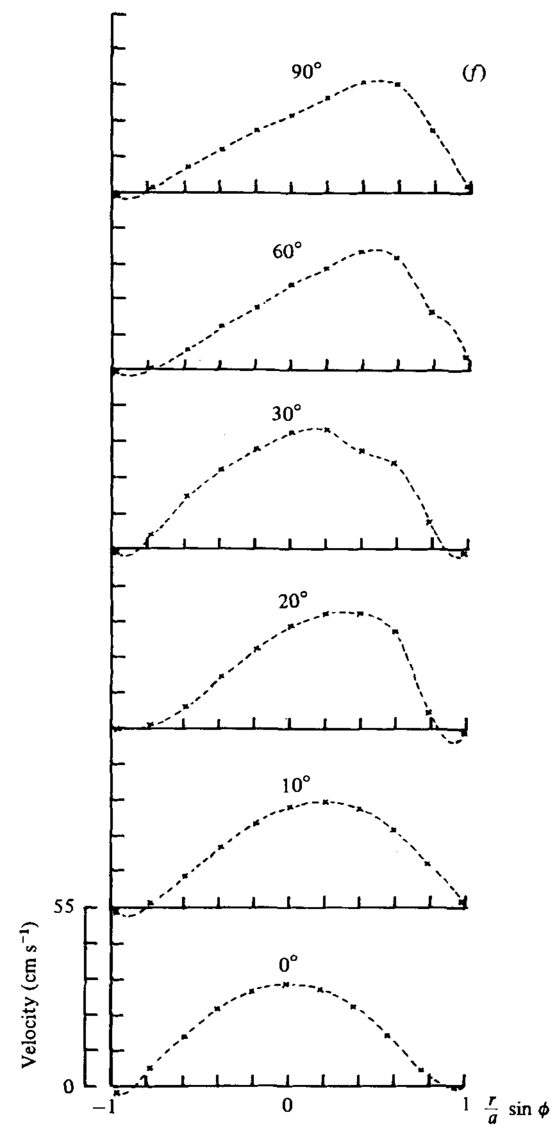


FIGURE 3. Experimental velocity profiles measured at various phase positions and at radial positions 0°–90° round the curve, to show the flow development around the bend when $\alpha = 4{\cdot}36$. Phase positions: (*a*) 0; (*b*) $\frac{1}{6}\pi$; (*c*) $\frac{1}{3}\pi$; (*d*) $\frac{1}{2}\pi$; (*e*) $\frac{2}{3}\pi$; (*f*) $\frac{5}{6}\pi$.

the direction of the skew in the axial velocity profile is not only controlled by the frequency parameter $\alpha$ but is also affected by the $D$ of the flow. This effect cannot be accounted for in the present perturbation scheme of part 2, which is only first order in $D$.

The final two phase positions presented concern the phase positions $\frac{2}{3}\pi$ and $\frac{5}{6}\pi$. Here viscous effects are important over the full width of the pipe and the development procedure is very similar to that found in the quasi-steady case. There is no observable downstream influence on the input profiles and the peaks drift directly to the outside of the bend under the action of the secondary flow. The development process takes a

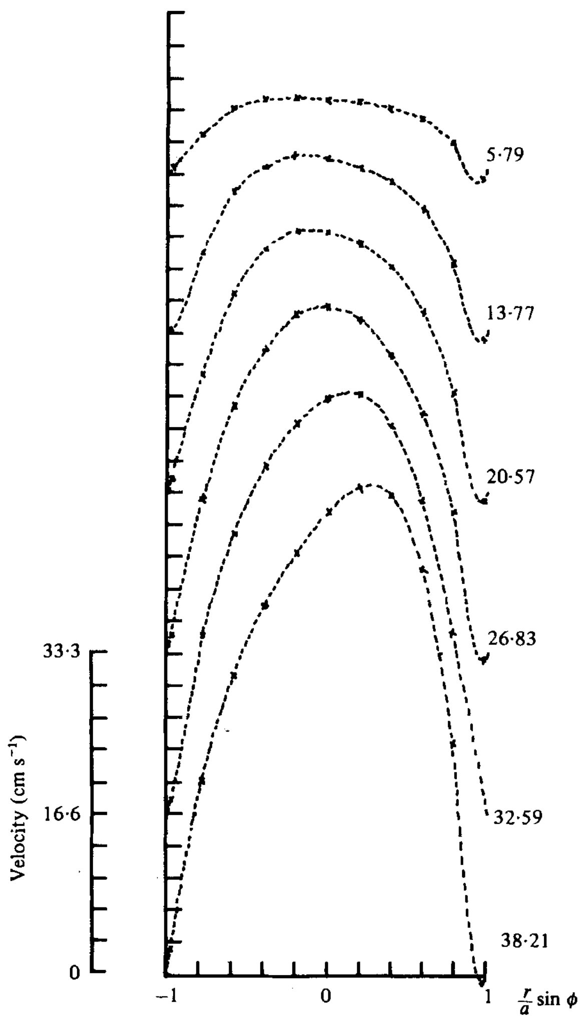


FIGURE 4. Series of profiles showing the effect of reducing $D$. Profiles measured at phase position $\frac{1}{2}\pi$ at 90° station round the curve with $\alpha = 4{\cdot}36$ and $D = 5{\cdot}79$–$38{\cdot}21$.

greater distance to complete in these cases than for the 0 and $\frac{1}{2}\pi$ phase positions, indicating the important role of viscosity, as was also found by Olsen.

Other results, generally confirming those presented here, may be found in Mullin (1978).

## 4. Conclusions

The most important conclusion which may be drawn from these results with regard to part 2 of this study is that essentially fully developed flow conditions apply at position 90° round the curve. The results used for the comparison with theory in part 2 were taken at a $D$ around $\frac{1}{4}$ times that used here for the cases $\alpha = 4{\cdot}36$, and thus fully developed flow is assured.

The development length is dependent upon the amount of vorticity in the input profile. This is in accordance with the earlier work of Gerrard & Hughes (1971) who studied the unsteady entry flow problem for a straight pipe. It is also in agreement with earlier steady-flow studies for the curved pipe.

The magnitude of the upstream influence due to the downstream curvature on the input profile is also strongly dependent upon the amount of vorticity in the incoming flow. When the incoming flow has a vorticity-free central core the upstream effect is pronounced. The modification of the initial flow to the fully developed steady-flow position depends upon the viscosity derived secondary flow overcoming the upstream influence.

As $\alpha$ increases, the regions where viscosity is important, and thus the regions where secondary flow is generated, are confined closer to the walls of the pipe. Within a cycle there is a slower build-up of secondary flow than the primary flow and thus for part of the cycle the axial velocity distribution retains its inward skew. The situation may be altered at larger $D$s where the effects described above may be obscured at the 'change-over' phase position.

T. Mullin acknowledges the support of the S.R.C. during the period of this work. Mr A. D. Molyneux is thanked for manufacturing most of the experimental apparatus used in this study.

## REFERENCES

AGRAWAL, Y., TALBOT, L. & GONG, K. 1978 Laser anemometer study of flow development in curved circular pipes. *J. Fluid Mech.* **85**, 497–518.

GERRARD, J. H. & HUGHES, M. D. 1971 The flow due to an oscillating piston in a cylindrical tube: a comparison between experiment and simple entrance flow theory. *J. Fluid Mech.* **50**, 97–106.

HUMPHREY, J. A. C. 1977 Flow in ducts with curvature and roughness. Ph.D. thesis, University of London.

HUMPHREY, J. A. C. & WHITELAW, J. H. 1976 Measurements in curved flows. *Proc. Squid Conf., Internal Flows, Airlie House.*

HUMPHREY, J. A. C., TAYLOR, A. M. K. & WHITELAW, J. H. 1977 Laminar flow in a square duct of strong curvature. *J. Fluid Mech.* **83**, 509–527.

ITO, H. 1961 Pressure losses in smooth pipe bends. *Rep. Inst. High Speed Mech., Japan* **12** (112), 41–62.

MULLIN, T. 1978 Oscillatory flow in curved tubes. Ph.D. thesis, University of Edinburgh.

MULLIN, T. & GREATED, C. A. 1978 Measurement of pulsating flows by photon-correlation. *J. Phys.* E, *Sci. Instrum.* **11**, 643–646.

MULLIN, T. & GREATED, C. A. 1980 Oscillatory flow in curved pipes. Part 2. The fully developed case. *J. Fluid Mech.* **98**, 397–416.

OLSON, D. E. 1971 Fluid mechanics relevant to respiration-flow within curved or elliptical tubes and bifurcating systems. Ph.D. thesis, University of London.

PRATAP, V. S. & SPALDING, D. B. 1975 Numerical computation of the flow in curved ducts. *Aero. Quart.* **26**, 219–228.

SINGH, M. P., SINHA, P. C. & AGGARWAL, M. 1978 Flow in the entrance of the aorta. *J. Fluid Mech.* **87**, 97–120.

SMITH, F. T. 1976 Fluid flow into a curved pipe. *Proc. Roy. Soc.* A **351**, 71–87.

UCHIDA, S. 1956 The pulsating viscous flow superposed on the steady motion of incompressible fluid in a circular pipe. *Z. angew. Math. Phys.* **7**, 403–421.

YAO, L. S. 1978 Entry flow in a heated straight pipe. *J. Fluid Mech.* **88**, 465–483.

YAO, L. S. & BERGER, S. A. 1975 Entry flow in a curved pipe. *J. Fluid Mech.* **67**, 177–196.